

Nonpropagating oscillatory modes in Couette-Taylor flow

Li-Hua Zhang* and Harry L. Swinney

Department of Physics, University of Texas, Austin, Texas 78712

(Received 26 July 1984)

We have made power-spectral measurements in both laboratory and rotating reference frames on fluid flow between rotating concentric cylinders. The oscillating modes identified in previous experiments were traveling azimuthal waves; in contrast, three of the oscillatory modes observed in the present experiment were found to be nonpropagating. One of the modes gives an instrumentally sharp component in the spectra, while the other two produce broad spectral components; hence the latter two flows are nonperiodic.

Previous studies of fluid flows in circularly symmetric systems have revealed a variety of states with traveling azimuthal waves. The best known example is wavy vortex flow between concentric rotating cylinders (the circular Couette system), studied extensively by Coles¹ and more recently by many others.²⁻⁴ In this flow there are traveling azimuthal waves on the toroidal ("Taylor") vortices that encircle the inner cylinder. Other examples of traveling waves in the circular Couette system include waves on the Taylor vortex-flow outflow boundaries,⁵ waves on the Taylor vortex-flow inflow boundaries,⁵ waves that appear as twists inside Taylor vortices which have stationary inflow and outflow boundaries,⁵ laminar spiral flow,⁶ and spiral turbulence.¹ Traveling azimuthal waves have also been observed in other circularly symmetric systems including a rigidly rotating annulus with a radial temperature gradient⁷ and concentric rotating spheres.⁸ We have found three examples of spectral components for Couette flow that do not correspond to traveling azimuthal waves. To our knowledge these are the first examples for circularly symmetric rotating fluids of oscillations that do not arise from traveling waves.

These nonpropagating modes occur over large ranges in Reynolds number R , axial wavelengths λ , and aspect ratios Γ : $3 \lesssim R/R_c \lesssim 10$; $2.0 \lesssim \lambda/d \lesssim 3.6$; and $10 \lesssim \Gamma$. (Γ is the ratio of the fluid height to the gap d between the cylinders; $R = 2\pi a d F_{\text{cyl}}/\nu$, where a is the inner cylinder radius, F_{cyl} the rotational frequency of the inner cylinder, and ν the kinematic viscosity; R_c is the Reynolds number corresponding to the onset of Taylor vortex flow.) We will now describe the apparatus and experimental methods, and then we will present and discuss the results.

Our concentric cylinder system, described in detail elsewhere,² has a radius ratio of 0.883 and an aspect ratio that can be adjusted from 0 to 50. The working fluid for these experiments was water with polymeric flakes (Kalliroscope AQ1000, 2% concentration) added for flow visualization and for the scattering intensity measurements. Most measurements were made with $\Gamma = 20$, the exact value being determined by the desired value of λ ; a few measurements were made for Γ as small as 10 and as large as 50. The lower fluid boundary was formed by a Teflon ring attached to the outer cylinder. For ease in adjustment of λ , the upper surface was left free in most

measurements, but some measurements were made using a Teflon ring as the upper boundary; no qualitative difference was found for the two cases. The intensity of laser light scattered from a small volume of the flow was recorded in a computer and then Fourier transformed to obtain power spectra.

For flows with spectra that consist of a single fundamental frequency and its harmonics it is easy to identify that fundamental with visually observed waves. However, when the spectra contain more than one fundamental frequency component, the character of the modes giving rise to the spectral components cannot in general be determined from time-series measurements at a single spatial point or from qualitative flow-visualization measurements.

We have identified the character of the modes giving rise to different spectral components by making measurements in both laboratory and rotating frames. The measurements in the rotating frame were made by mounting the apparatus on a rotating table³ that is coaxial with the Couette system. The speeds of the Couette cylinder and the rotating table are controlled entirely independently.

For traveling azimuthal waves the measurements in a rotating reference frame readily yield both the number of waves around the annulus and the rotation frequency of the waves. We will illustrate this with data obtained for a flow in which there are both stationary oscillatory modes and a traveling azimuthal wave. Consider a traveling wave with a phase angle θ in the laboratory reference frame and phase θ' in a reference frame that rotates with frequency F_r . Then

$$\theta' = \theta - 2\pi F_r t . \quad (1)$$

Hence the frequency f observed in spectra of the scattered light intensity obtained in the laboratory reference frame and f' observed in spectra obtained in the rotating frame are related by

$$f' = f - m F_r , \quad (2)$$

where m is the number of waves around the annulus. Graphs of f' versus F_r then yield m from the slope and the wave speed f/m from the $f' = 0$ intercept.

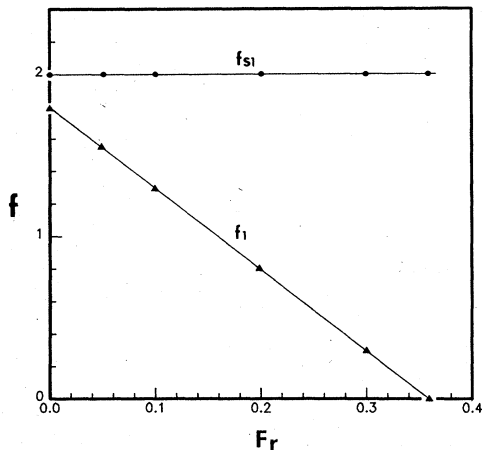


FIG. 1. Frequencies of two of the observed spectral components are shown as a function of the reference-frame rotation frequency F_r : f_1 corresponds to a traveling azimuthal wave with five waves around the annulus and f_{s1} to a stationary oscillatory mode. The frequencies are expressed relative to the cylinder frequency. Some of the spectra used to determine these frequencies are shown in Fig. 2.

The observed frequencies of the two spectral components are graphed in Fig. 1 as a function of the reference-frame rotation frequency. For f_1 the observed frequency decreases linearly with F_r , indicating that f_1 corresponds to a *traveling wave* which rotates in the same direction as the rotating reference frame. The slope of the line is -4.9997 ± 0.0004 ; hence there are five waves around the annulus. The $f'=0$ intercept yields the wave rotation frequency $f_1/m = 0.3591 \pm 0.0002$.

The behavior of the second frequency plotted in Fig. 1., f_{s1} , is quite different—it is *independent* of F_r . The difference in the behavior of f_1 and f_{s1} is clear from Fig. 2, which shows power spectra obtained in the laboratory and rotating reference frames. In Fig. 2 there are two fundamental frequencies that correspond to stationary modes: f_{s1} , which is sharp, and f_{s2} , which is broad. Although f_{s1} and f_{s2} appear to be centered at about the same frequency in Fig. 2, measurements for a large range of control parameters have made it clear that f_{s1} and f_{s2} correspond to distinct modes.⁹ For example, in Fig. 3(a), f_{s2} is clearly centered at a higher frequency than f_{s1} . In Fig. 3(b), f_{s1} is fairly intense and f_{s2} is not observed, but another broad spectral component, f_{s3} , corresponding to another stationary mode, is present.

The spectral components called f_{s1} , f_{s2} , and f_{s3} were examined over large ranges in R , λ , and Γ , and for different positions of the laser-beam probe in the fluid. In all cases the observed frequencies were found to be independent of the rotation frequency of the reference frame. Thus these frequencies are *stationary oscillations*, not traveling azimuthal waves.

The intensity of the nonpropagating modes varies strongly with axial position. These modes were not observable in spectra obtained at or very near a vortex inflow boundary, but the modes were observable at all other

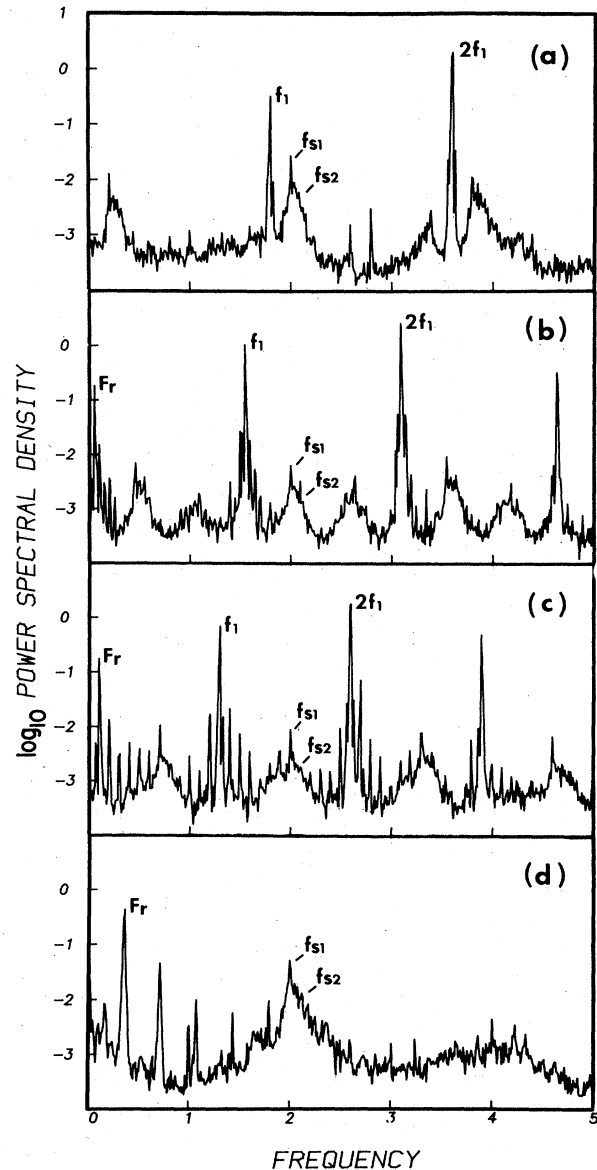


FIG. 2. Four spectra obtained for different reference-frame rotation frequencies for the same flow: (a) $F_r=0$ (the laboratory reference frame), (b) $F_r=0.050$, (c) $F_r=0.10$, and (d) $F_r=0.359$ (the co-moving frame for f_1). One component (f_1) and its harmonics correspond to a traveling azimuthal wave. Two components, one sharp (f_{s1}) and one broad (f_{s2}), correspond to stationary oscillatory modes. The components at F_r and F_{cyl} [$F_{\text{cyl}} \equiv 1$; see (c) and (d)] are instrumental artifacts arising from variations in the reflectivity of the inner cylinder and imperfections on the outer wall of the glass outer cylinder (not the wall in contact with the fluid).⁹ The spectra were obtained at $R/R_c=7.0$ with $\lambda/d=2.95$ and $\Gamma=22.1$.

positions in the vortices, including the vortex outflow boundaries. The intensity was greatest near the center of the vortices.

Oscillations in the flow pattern at frequencies f_{s1} or f_{s2} and at f_{s3} were observed visually in the co-rotating frame

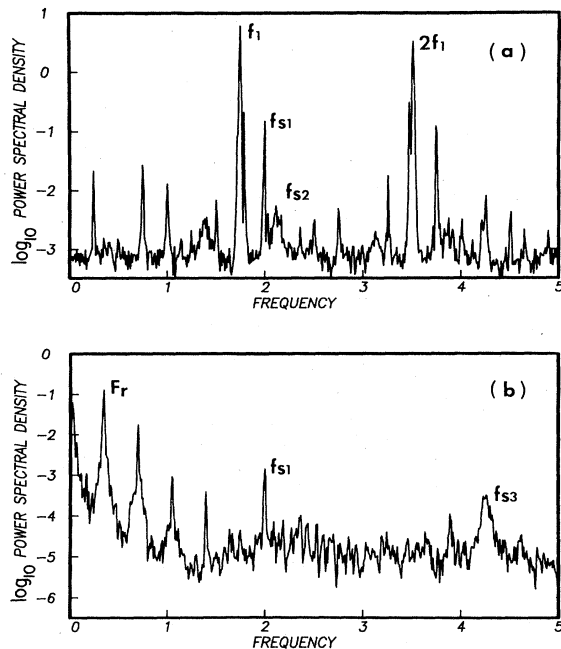


FIG. 3. (a) A power spectrum in which the frequency components f_{s1} and f_{s2} are centered at different frequencies. The component f_{s3} is weak or absent. ($F_r=0$, $R/R_c=7.0$, $\lambda/d=2.4$, and $\Gamma=20.0$.) (b) A power spectrum containing f_{s1} and f_{s3} ; f_{s2} is weak or absent. The spectrum was obtained at a point near the stability boundary in Fig. 5. ($F_r=0.35$, $R/R_c=6.5$, $\lambda/d=2.1$, and $\Gamma=22.1$.)

of the azimuthal wave f_1 . The oscillations are rather weak, as Fig. 4 illustrates. The different modes were identified by comparing the periods measured with a stopwatch in visual observations with the frequencies in the spectra. The oscillations in successive Taylor vortex pairs appear to be in phase.

The amplitudes and frequencies of the stationary modes f_{s1} and f_{s2} were examined as a function of aspect ratio at $R/R_c=7.0$ and $\lambda/d=3.1$. When Γ was reduced below

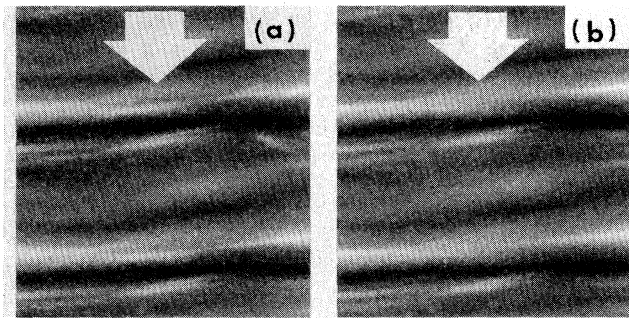


FIG. 4. These photographs, obtained in the co-moving reference frame of the azimuthal wave f_1 , show the nonpropagating oscillatory mode f_{s3} . The time difference between the photographs is $0.43/f_{s3}$. The flow pattern in the region marked by the arrows has a sharp bright line in (a) which becomes diffuse in (b). ($m=5$, $R/R_c=8.5$, $\lambda/d=2.4$, and $\Gamma=22.9$.)

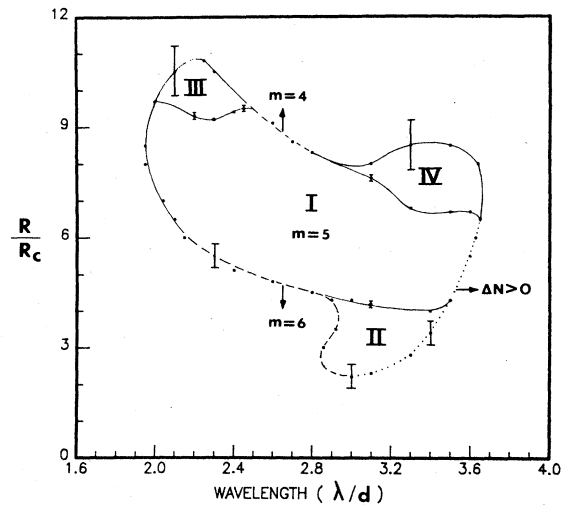


FIG. 5. The domain of stationary oscillatory modes for a wavy-vortex-flow state with five waves. (Γ was adjusted within the range $19.0 < \Gamma < 23.4$ to obtain the desired λ .) The mode f_{s1} is stable inside all the regions I-IV, the mode f_{s2} inside I, and the mode f_{s3} inside regions I, II, and III. The upper and lower dashed boundaries mark transitions in the number of waves; the dotted curve marks transitions at which the number of vortices increases. Error bars are shown for a few representative points.

17, the amplitude of f_{s2} became very small and finally, for $\Gamma \leq 10$, unobservable; f_{s1} remained observable even for $\Gamma < 10$. When Γ was increased from 20 to more than 40, no significant change in the amplitudes of f_{s1} and f_{s2} was observed. The frequencies f_{s1} and f_{s2} were independent of Γ .

Figure 5 shows the domains of stability of the stationary oscillatory modes. The stability boundaries were determined by holding λ (i.e., Γ) fixed and increasing or decreasing R until a state lost stability.¹⁰ At the left-hand boundary the amplitude of f_{s2} goes to zero continuously, while the amplitudes of f_{s1} and f_{s3} remain large until the stability boundary is reached. At the right-hand stability boundary there is a transition at which another vortex pair forms within the annulus. At the part of the upper boundary marked by the dashed line there is a transition from an $m=5$ to an $m=4$ state; similarly, the stationary modes disappear at the lower boundary, at which there is a transition from an $m=5$ to an $m=6$ state. The transitions at the upper, lower, and right-hand boundaries of the stability region for the stationary oscillatory modes all exhibit hysteresis. The modes f_{s1} and f_{s2} were always present in the regions indicated in Fig. 5, while f_{s3} was not as reproducible—it was sometimes absent under the same conditions in which it was usually observed.

These stationary oscillatory modes occur at low Reynolds numbers where accurate numerical simulations are possible.¹¹ A simulation of the nonperiodic stationary modes would be particularly interesting. The stationary modes could exhibit an infinite period-doubling sequence (Feigenbaum cascade), which is not possible for traveling waves, at least not by means of sequential halving of the

number of azimuthal waves; such a period-doubling sequence has in fact been recently observed by Pfister¹² in a Couette-Taylor system with a radius ratio of 0.5 and a very small aspect ratio (0.5).

There are many unanswered questions about the stationary modes that should be examined in future studies. For example, is this flow described by a low dimensional strange attractor? How do the dimension and Lyapunov exponents vary with R , λ , and Γ ?¹³

ACKNOWLEDGMENTS

We thank C. D. Andereck, who designed the rotating-table system, and A. Brandstätter for their advice and assistance. This research is supported by National Science Foundation Fluid Mechanics Program Grant No. MEA-82-06889. One of us (H.L.S.) acknowledges the support by the Guggenheim Foundation.

*Permanent address: Institute of Physics, Chinese Academy of Sciences, Beijing, China.

¹D. Coles, *J. Fluid Mech.* **21**, 385 (1965).

²M. Gorman and H. L. Swinney, *J. Fluid Mech.* **117**, 123 (1982).

³R. S. Shaw, C. D. Andereck, L. A. Reith, and H. L. Swinney, *Phys. Rev. Lett.* **48**, 1172 (1982).

⁴See also, e.g., T. Mullin and T. Brooke Benjamin, *Nature* **288**, 567 (1980); G. Pfister and U. Gerds, *Phys. Lett.* **83A**, 23 (1981); G. Ahlers, D. S. Cannell, and M. A. Dominguez-Lerma, *Phys. Rev. A* **27**, 1225 (1983); K. Park, G. L. Crawford, and R. J. Donnelly, *Phys. Rev. Lett.* **51**, 1352 (1983).

⁵C. D. Andereck, R. Dickman, and H. L. Swinney, *Phys. Fluids* **26**, 1395 (1983).

⁶H. A. Snyder, *Phys. Fluids* **11**, 728 (1968).

⁷R. Hide, P. J. Mason, and R. A. Plumb, *J. Atmos. Sci.* **34**, 930 (1977).

⁸M. Wimmer, *J. Fluid Mech.* **78**, 317 (1976); I. M. Yavorskaya,

Yu. N. Belyaev, A. A. Monakhov, N. M. Astaf'eva, S. A. Scherbakov, N. D. Vvedenskaya, in *Proceedings of the XVth International Congress of Theoretical and Applied Mechanics, 1980* (North-Holland, Amsterdam, 1981), p. 431; Yu. N. Belyaev and I. M. Yavorskaya, in *Nonlinear Dynamics and Turbulence*, edited by G. I. Barenblatt, G. Iooss, and D. D. Joseph (Pittman, New York, 1983).

⁹Although f_{s1} and f_{s2} are about equal to $2F_{\text{cyl}}$, their independence of F , makes it clear that they are not artifacts related to the rotation of the cylinder.

¹⁰G. P. King and H. L. Swinney, *Phys. Rev. A* **27**, 1240 (1983).

¹¹P. S. Marcus, *J. Fluid Mech.* **146**, 45 (1984); P. S. Marcus, *J. Fluid Mech.*, **146**, 65 (1984).

¹²G. Pfister, to appear.

¹³A. Brandstätter, J. Swift, H. L. Swinney, A. Wolf, J. D. Farmer, E. Jen, and J. P. Crutchfield, *Phys. Rev. Lett.* **51**, 1442 (1983).

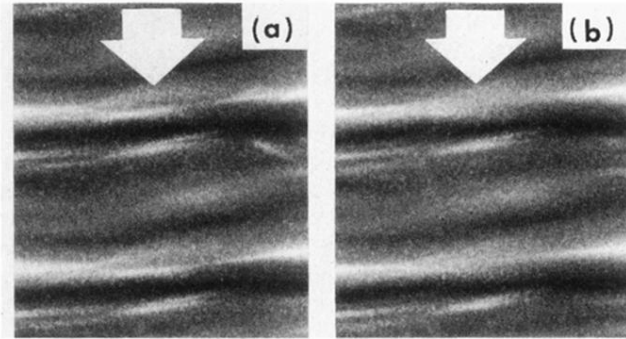


FIG. 4. These photographs, obtained in the co-moving reference frame of the azimuthal wave f_1 , show the nonpropagating oscillatory mode f_{s3} . The time difference between the photographs is $0.43/f_{s3}$. The flow pattern in the region marked by the arrows has a sharp bright line in (a) which becomes diffuse in (b). ($m = 5$, $R/R_c = 8.5$, $\lambda/d = 2.4$, and $\Gamma = 22.9$.)